Article

TRANSPARENT PROCESS

THE EMBO JOURNAL

An LXR–NCOA5 gene regulatory complex directs inflammatory crosstalk-dependent repression of macrophage cholesterol efflux

Mark A Gillespie[1], Elizabeth S Gold[2], Stephen A Ramsey[3], Irina Podolsky[2], Alan Aderem[2] & Jeffrey A Ranish[1,*]

Abstract

LXR–cofactor complexes activate the gene expression program responsible for cholesterol efflux in macrophages. Inflammation antagonizes this program, resulting in foam cell formation and atherosclerosis; however, the molecular mechanisms underlying this antagonism remain to be fully elucidated. We use promoter enrichment-quantitative mass spectrometry (PE-QMS) to characterize the composition of gene regulatory complexes assembled at the promoter of the lipid transporter *Abca1* following downregulation of its expression. We identify a subset of proteins that show LXR ligand- and binding-dependent association with the *Abca1* promoter and demonstrate they differentially control *Abca1* expression. We determine that NCOA5 is linked to inflammatory Toll-like receptor (TLR) signaling and establish that NCOA5 functions as an LXR corepressor to attenuate *Abca1* expression. Importantly, TLR3–LXR signal crosstalk promotes recruitment of NCOA5 to the *Abca1* promoter together with loss of RNA polymerase II and reduced cholesterol efflux. Together, these data significantly expand our knowledge of regulatory inputs impinging on the *Abca1* promoter and indicate a central role for NCOA5 in mediating crosstalk between pro-inflammatory and anti-inflammatory pathways that results in repression of macrophage cholesterol efflux.

Keywords atherosclerosis; inflammation; LXR; NCOA5; quantitative mass spectrometry

Subject Categories Immunology; Metabolism

DOI 10.15252/embj.201489819 | Received 15 August 2014 | Revised 11 February 2015 | Accepted 13 February 2015 | Published online 9 March 2015

The EMBO Journal (2015) 34: 1244–1258

Introduction

Macrophages have a critical role in maintaining systemic lipid homeostasis. They promote the efflux of excess intracellular cholesterol to high-density lipoproteins (HDL), thereby facilitating its return to the liver through the reverse cholesterol transport system. Macrophage cholesterol efflux is dependent on membrane-associated lipid transporters, such as ATP-binding cassette, subfamily A, member 1 (ABCA1) (Oram *et al*, 2000; Vaisman *et al*, 2001; Wang *et al*, 2007; Yvan-Charvet *et al*, 2007). The importance of ABCA1 function to this process is illustrated in Tangier disease, where mutations in the *Abca1* gene disrupt cholesterol efflux resulting in the formation of lipid-filled macrophage foam cells (Bodzioch *et al*, 1999; Brooks-Wilson *et al*, 1999; Rust *et al*, 1999; Orso *et al*, 2000).

Macrophage foam cells are highly prevalent and significant contributors to the pathology of the chronic inflammatory disease atherosclerosis, a leading cause of morbidity and mortality worldwide (Moore *et al*, 2013; http://www.who.int/mediacentre/factsheets/fs317/en/). During the development of atherosclerosis, extrinsic inflammatory stimuli activate pro-inflammatory macrophage Toll-like receptors (TLRs), which repress expression of lipid transporters, and therefore impede cholesterol efflux (Castrillo *et al*, 2003; Spann *et al*, 2012). Notably, in mice, the absence of *Abca1* expression in macrophages results in increased foam cell formation and atherosclerosis (Aiello *et al*, 2002; van Eck *et al*, 2002), while in humans, loss of macrophage cholesterol efflux capacity is a significant risk factor for atherosclerosis (Khera *et al*, 2011). In fact, therapeutic efforts are now focused on enhancing macrophage cholesterol efflux capacity in atherosclerosis (Rader & Tall, 2012), signifying the importance of understanding the molecular regulation of lipid transporter expression.

The central regulators of lipid transporter expression are the sterol sensing liver X receptor (LXR) transcription factors LXRα (*Nr1h3*) and LXRβ (*Nr1h2*). LXRs heterodimerize with retinoid X receptors (RXRs), and upon binding to regulatory sites for the lipid transporters *Abca1* and *Abcg1*, the LXR–RXR complex induces transcription in a sterol ligand-dependent manner (Costet *et al*, 2000; Repa *et al*, 2000; Venkateswaran *et al*, 2000a,b). As a result, sterol ligand stimulation of LXRs inhibits atherosclerotic plaque formation in mice (Joseph *et al*, 2002). The specificity of this sterol-mediated

1 Institute for Systems Biology, Seattle, WA, USA
2 Seattle Biomedical Research Institute, Seattle, WA, USA
3 Department of Biomedical Sciences, Oregon State University, Corvallis, OR, USA
*Corresponding author. Tel: +1 206 732 1357; Fax: +1 206 732 1299; E-mail: jeff.ranish@systemsbiology.org

gene induction is dependent on LXR–cofactor interactions, where corepressor complexes are replaced with coactivator complexes (Wagner *et al*, 2003; Huuskonen *et al*, 2004, 2005; Lee *et al*, 2008; Jakobsson *et al*, 2009). However, the full compendium of these signal-dependent interactions at the regulatory regions of lipid transport genes remains to be elucidated.

Interestingly, the anti-inflammatory LXRs and pro-inflammatory TLRs antagonize each other in macrophages (Castrillo *et al*, 2003; Joseph *et al*, 2003; Ogawa *et al*, 2005). LXRs prevent induction of pro-inflammatory gene expression through sumoylation-dependent transrepression (Ogawa *et al*, 2005; Ghisletti *et al*, 2007; Huang *et al*, 2011). Conversely, TLR3-4 signaling represses LXR-dependent gene activation (Castrillo *et al*, 2003). In atherosclerosis, the pro-inflammatory pathway appears dominant over the anti-inflammatory LXR pathway, resulting in reduced macrophage cholesterol efflux and foam cell formation. While these observations indicate the importance of signal crosstalk, much remains to be understood about the mechanisms governing these interactions and their effects on lipid transporter expression.

We hypothesized that activation of the TLR3 pathway downregulates LXR-mediated cholesterol efflux by recruiting corepressors to, or maintaining corepressors on, the promoters of lipid transporter genes. To identify such factors, we employed promoter enrichment-quantitative mass spectrometry (PE-QMS) to characterize the composition of gene regulatory complexes at the *Abca1* promoter (Ranish *et al*, 2003, 2004; Kim *et al*, 2007; Mittler *et al*, 2009; Foulds *et al*, 2013; Mirzaei *et al*, 2013; Viturawong *et al*, 2013). We performed a systems-level analysis of proteins that associate with *Abca1* regulatory DNA in macrophages at a time when *Abca1* expression was being downregulated, as these are likely to reflect corepressor interactions. Using quantitative mass spectrometry, we simultaneously identified a compendium of LXR ligand-stimulated and LXR binding-dependent regulators, including the nuclear receptor cofactor NCOA5. We further demonstrate that NCOA5 is recruited to the *Abca1* promoter *in vivo* in response to both lipid and inflammatory signals where it functions as an LXR corepressor to suppress *Abca1* transcription and cholesterol efflux.

Results

Identification of LXR-dependent transcriptional regulators using promoter enrichment-quantitative mass spectrometry (PE-QMS)

To investigate the mechanisms controlling *Abca1* transcription, we began by examining its expression dynamics in response to the synthetic LXR ligand T0901317 (Schultz *et al*, 2000). Using isolated C57BL/6 bone marrow-derived primary macrophages (BMMs), we observed an initial ligand-stimulated increase in both *Abca1* mRNA (Fig 1A) and ABCA1 protein (Supplementary Fig S1A and B). This response was dependent on LXR, as *Nr1h3*$^{-/-}$:*Nr1h2*$^{-/-}$ (LXR$^{-/-}$) BMMs failed to induce ligand-stimulated expression (Fig 1A). We also observed minimal changes in *Nr1h3* and *Nr1h2* mRNA expression during this response (Supplementary Fig S1C and D).

Notably, *Abca1* ligand-stimulated mRNA expression peaked at 8–16 h and was subsequently followed by a decline in expression in LXR$^{+/+}$ BMMs (Fig 1A). We observed a similar pattern in ABCA1 protein expression (Supplementary Fig S1A). While current evidence suggests LXR coactivators are responsible for ligand-stimulated transcriptional induction (Calkin & Tontonoz, 2012), a mechanism to explain the subsequent attenuation of the *Abca1* transcriptional response following ligand treatment remains unknown (Fig 1A).

To test the hypothesis that LXR cofactor complexes are responsible for attenuating *Abca1* expression in macrophages, we undertook a multifaceted approach to compare *Abca1* promoter-associated proteins using promoter enrichment-quantitative mass spectrometry (PE-QMS) (Fig 1B). PE-QMS uses *in vitro* biotinylated regulatory DNA to enrich for gene regulatory complexes, which are subsequently identified and quantified by mass spectrometry. Notably, this technology requires no *a priori* knowledge of transcription factor binding. We chose a 321-bp genomic regulatory sequence flanking the proximal direct repeat 4 (DR4) LXR response element (LXRE) of *Abca1*, which contains the TATA box and is responsive to LXR ligand stimulation (Supplementary Fig S2A). Importantly, this sequence is within a DNaseI hypersensitive region and is devoid of nucleosomes, as measured by DNase-Seq and acetylated histone H4 ChIP-seq, respectively (Supplementary Fig S2B) (Ramsey *et al*, 2010; Gold *et al*, 2012).

To isolate and identify transcriptional regulators which bind to this region in an LXR ligand-stimulated manner, nuclear extracts from RAW 264.7 macrophages stimulated for 18 h with LXR ligand or vehicle control were incubated with the biotinylated *Abca1* regulatory sequence, and stably bound proteins were eluted and analyzed by quantitative mass spectrometry (Fig 1B). These macrophages displayed a similar response to the synthetic LXR ligand T0901317 as primary BMMs (Supplementary Fig S3). To determine which of these associations were dependent on LXR promoter binding, we performed another PE-QMS experiment in which we compared the compendium of proteins bound to the wild-type LXRE in the *Abca1* promoter with those bound to an LXRE that we engineered to contain mutations that completely abolished LXR binding and the ligand-stimulated transcriptional response of *Abca1* (Fig 1B; Supplementary Figs S4 and S5).

After removing any proteins encoded by genes that were not expressed in primary macrophages (Ramsey *et al*, 2008; Gold *et al*, 2012), we identified 79 potential *Abca1* promoter-associated proteins (FDR < 1%; Fig 1C; Supplementary Table S1A and B). Using a 1.5-fold change in binding response as a cutoff, which we chose after examining the binding response of LXR and RXR, we identified ligand-stimulated and LXR-dependent subsets of interactions (Fig 1C; Supplementary Table S1C). Notably, these subsets were enriched for gene ontology (GO) terms related to transcription (Supplementary Table S2A–C).

We detected 19 proteins that were reproducibly enriched in the ligand-stimulated experiments, of which seven were dependent on LXR promoter binding, ten were independent, and two were undetermined (Fig 1C; Supplementary Table S1C). Interestingly, of these 19 ligand-stimulated associations, 15 were the products of genes whose RNA levels in macrophages did not change more than 1.5-fold in response to T0901317 (Supplementary Fig S6). Furthermore, all seven LXR-dependent associations, along with five of the LXR-independent associations, were from proteins annotated as transcription factors (Supplementary Table S1C) (Ashburner *et al*, 2000; Roach *et al*, 2007).

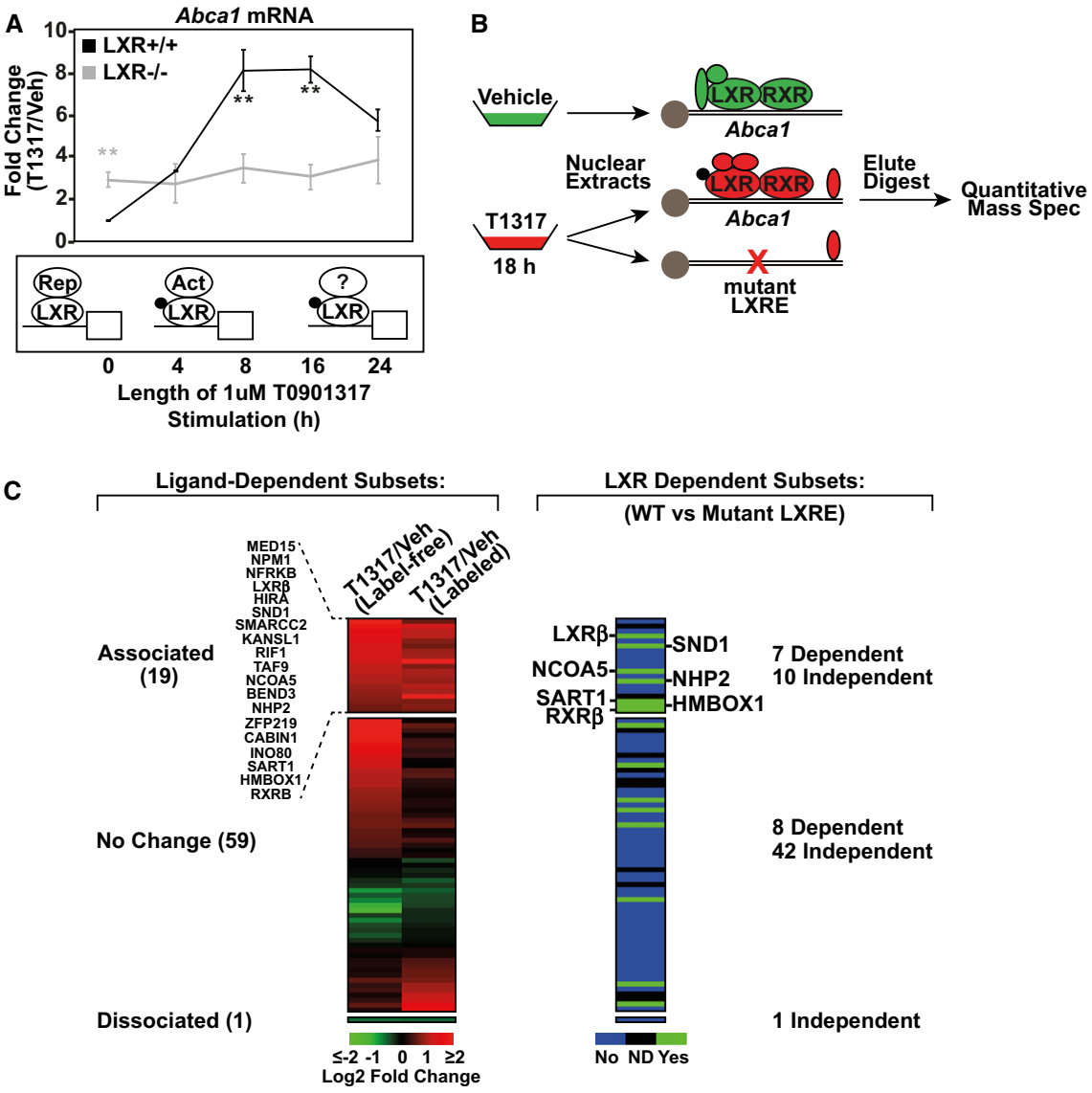

Figure 1. Promoter enrichment-quantitative mass spectrometry (PE-QMS) identifies transcriptional regulators of *Abca1* expression.

A RT–qPCR of *Abca1* transcripts following 1 μM T0901317 stimulation of $LXR^{+/+}$ and $LXR^{-/-}$ primary BMMs. Fold changes are shown relative to $LXR^{+/+}$ 0 h. Error bars represent ± SEM for n = 4–8 (**P = 0.001 at 8 h and **P = 0.00004 at 16 h versus $LXR^{-/-}$; **P = 0.0003 at 0 h versus $LXR^{+/+}$); bottom, proposed model explaining the ligand-dependent induction of *Abca1*. Following ligand stimulation, LXR–corepressor complexes are exchanged for LXR–coactivator complexes, which promote gene expression. The LXR–cofactor interactions responsible for the attenuation of expression beginning after 16 h remain unknown.

B Overview of the PE-QMS experimental strategy to identify LXR ligand-stimulated and LXR binding-dependent interactions with the *Abca1* promoter. Nuclear extracts were prepared from RAW 264.7 macrophages treated with control or 1 μM T0901317 (depicted as a black circle) for 18 h. The *Abca1* promoter region was used to isolate gene regulatory complexes under the indicated conditions. Immobilized templates were washed, and bound proteins eluted and digested. Peptides were purified, then identified, and quantified by mass spectrometry.

C Heat map of the PE-QMS experiment. Ligand-dependent subsets were quantified using label-free and isotope labeling approaches and are indicated on the left. Colors represent Log2 relative abundance ratios (T0901317/vehicle) of identified proteins. LXR binding-dependent subsets were quantified using an isotope labeling approach and are indicated on the right. Changes in binding > 1.5-fold were employed as cutoffs for depicted subsets. ND = not determined. Full dataset is available as Supplementary Table S1.

Functional validation of the ligand-stimulated and LXR-dependent candidate regulators

We next sought to assess the function of these LXR-dependent putative regulators identified by PE-QMS. We began by generating a protein interaction network *in silico*. This analysis indicated that both NCOA5 and NHP2 were connected to TLR-dependent inflammation through physical protein–protein interactions in mouse or human (Fig 2A). Moreover, reporter assays using the same regulatory sequence as that used for the PE-QMS enrichment indicated

that while SND1, SART1, and HMBOX1 induced *Abca1* transcription almost twofold ($P < 0.05$; Fig 2B), NCOA5 expression significantly repressed the *Abca1* transcriptional response threefold ($P = 0.00005$; Fig 2C). These results suggest a regulatory balance between activators and repressors functions to coordinate *Abca1* expression.

Interestingly, NCOA5 has previously been described as a cofactor for a small subset of nuclear receptors, including estrogen receptor 1 (ESR1); however, its role in transcription seems to be context dependent (Sauve *et al*, 2001; Jiang *et al*, 2004; Gao *et al*, 2013; Sarachana & Hu, 2013). In addition, polymorphisms in *Ncoa5* are associated with both chronic inflammatory disease and metabolic disease (Bento *et al*, 2008; Lewis *et al*, 2010; Zervou *et al*, 2011). To our knowledge, NCOA5 has never previously been implicated in LXR-regulated gene expression, cholesterol efflux, or atherosclerosis. This, together with its repression of *Abca1* transcription and its potential involvement in TLR signaling, makes NCOA5 an ideal candidate for further investigation.

NCOA5 functions as an LXR corepressor

To further investigate the role of NCOA5 in *Abca1* transcription, we performed reporter assays using NCOA5 and *Abca1* mutants. Deletion of the NH_2-terminus (Δ1–280aa), which contains a putative repressor domain (Sauve *et al*, 2001), abolished the repressive effect of NCOA5 on the reporter (Fig 2C). However, NCOA5 retained repressive activity after mutation of the LXRE (Fig 2C), suggesting it can still function in the absence of LXR binding. In addition, overexpression of NCOA5 in primary BMMs confirmed its ability to repress *Abca1* expression (Fig 2D; Supplementary Fig S7A).

To determine whether NCOA5 directly interacts with LXR, we performed *in vitro* pulldown assays. Full-length *in vitro* translated

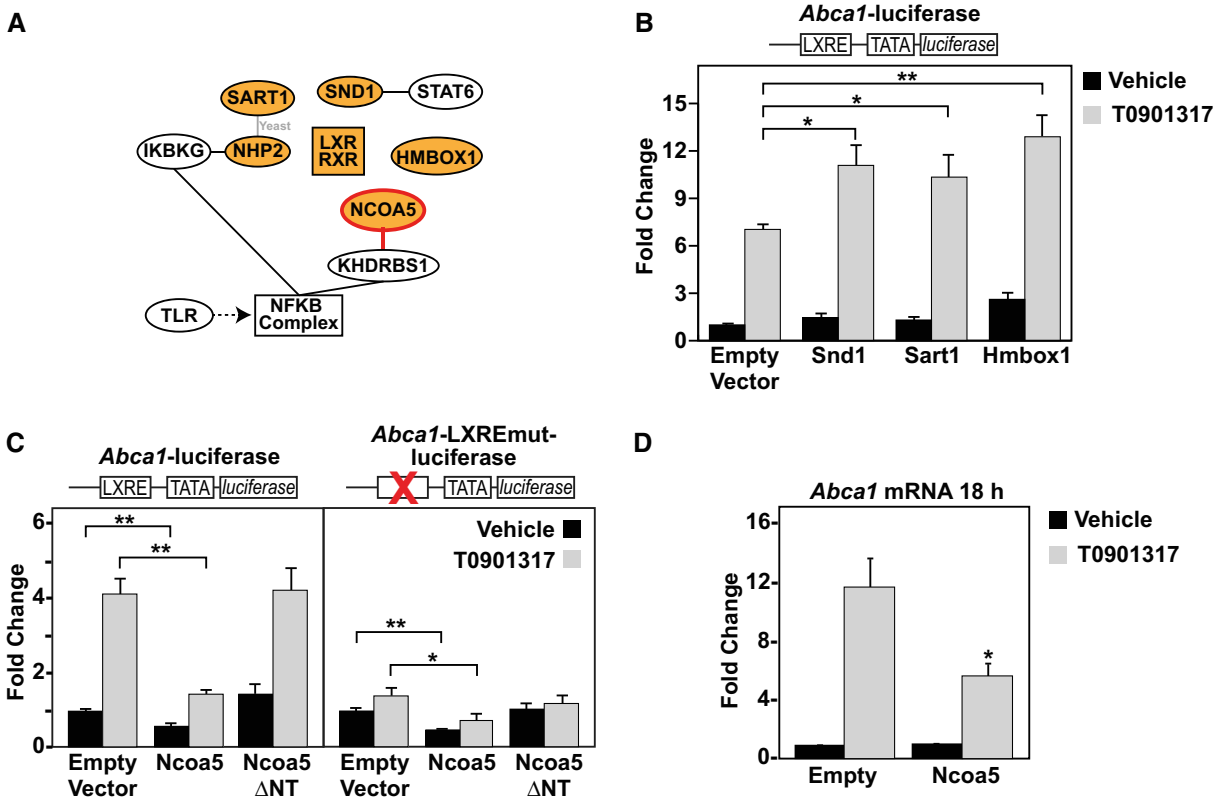

Figure 2. Identification of NCOA5 as an LXR repressor.

A Protein–protein interaction network showing connectivity between the putative ligand-stimulated and LXR binding-dependent transcriptional regulators of *Abca1* (shown in orange). Edges represent protein–protein interactions. NCOA5 node and edge are outlined red to indicate that this physical association is found in mouse interaction networks.

B Luciferase reporter assays from RAW 264.7 macrophages expressing reporter alone, or together with full-length SND1, SART1, or HMBOX1. LXR ligand stimulations with 1 μM T0901317 were performed for 18 h. A diagram of the reporter construct is shown above. Fold changes are shown relative to vehicle-stimulated reporter alone (first lane). Error bars represent ± SEM for $n = 9$ (**$P = 0.001$, *$P = 0.011$ for SND1, *$P = 0.046$ for SART1).

C Luciferase reporter assays from RAW 264.7 macrophages expressing reporter alone, or together with full-length NCOA5 or an NCOA5 mutant lacking the NH_2-terminus. LXR ligand stimulations with 1 μM T0901317 were performed for 18 h. Diagrams of the reporter constructs are shown above. Fold changes are shown relative to vehicle-stimulated reporter alone (first lane). Error bars represent ± SEM for $n = 6$–12 (**$P < 0.001$, *$P = 0.035$).

D RT–qPCR of *Abca1* transcripts following infection of primary BMMs with Ncoa5 or control retrovirus. LXR ligand stimulations were performed with 1 μM T0901317 for 18 h. Fold changes are shown relative to vehicle-stimulated control. Error bars represent ± SEM for $n = 4$ (*$P = 0.029$).

NCOA5 protein specifically bound to GST-LXRα in a ligand-independent manner (Fig 3A). Notably, deletion of the NH_2-terminus (Δ1–280aa) prevented this interaction, while the NH_2-terminal fragment strongly bound GST-LXRα (Fig 3A). Given the nuclear receptor interaction motif on NCOA5 is found within its COOH-terminus (Sauve *et al*, 2001), these results indicate NCOA5 directly interacts with LXR through a non-canonical domain in the NH_2-terminus.

To confirm that NCOA5 functions as an LXR cofactor, we examined their interaction in macrophage nuclear extracts. Indeed, endogenous NCOA5 immunoprecipitated with a Protein C-tagged version of LXRα expressed in RAW 264.7 macrophages (Fig 3B). Similar to the *in vitro* pulldowns, this *in vivo* interaction also occurred both in the presence and absence of LXR ligand. Together, these results indicate that NCOA5 functions as an LXR corepressor, and its mode of interaction appears to be distinct from its mode of interaction with ESR1 (Sauve *et al*, 2001).

To determine whether NCOA5 localizes to the *Abca1* promoter *in vivo*, we performed chromatin IP (ChIP) assays in primary BMMs

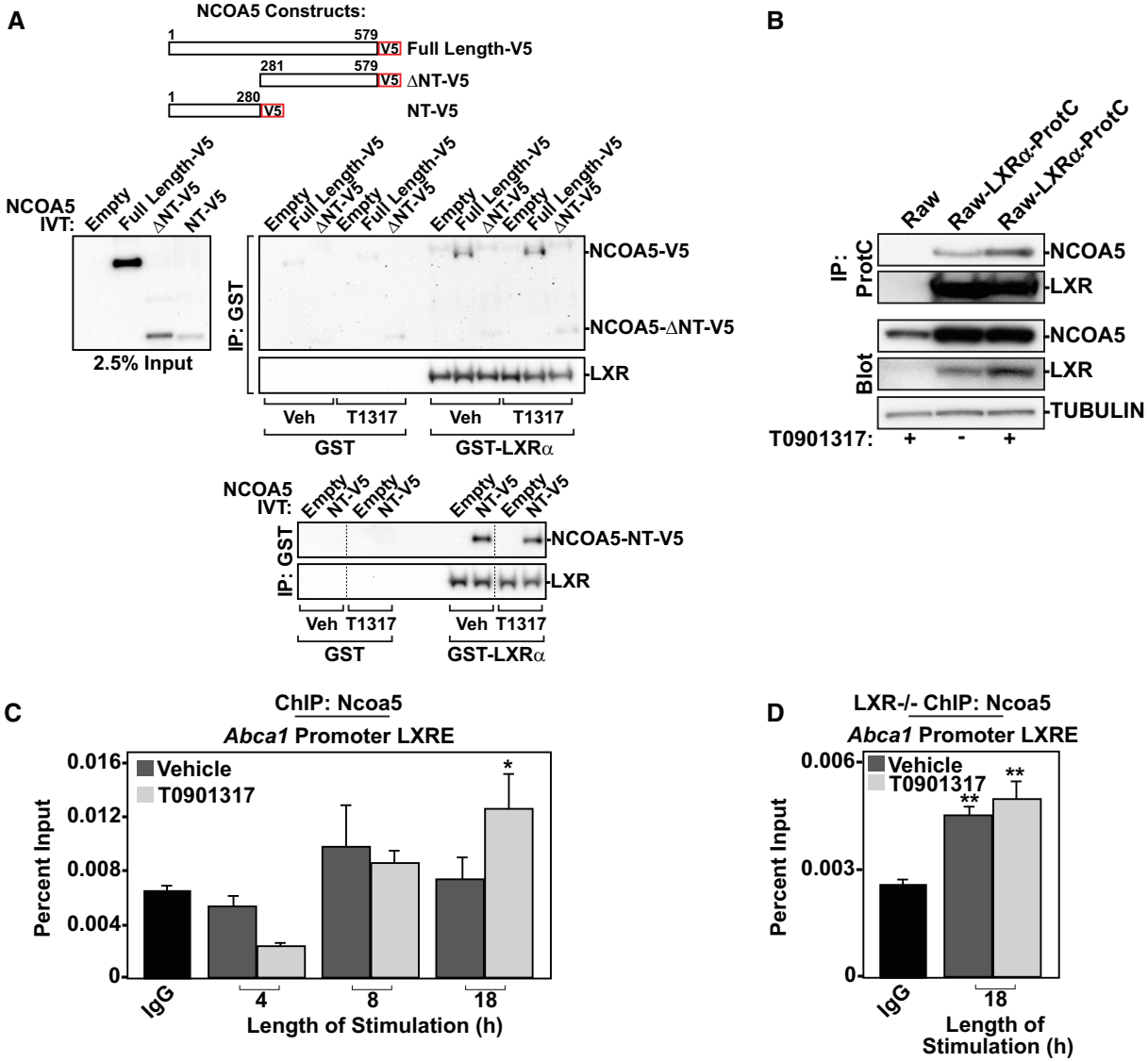

Figure 3. NCOA5 functions as an LXR corepressor.

A *In vitro* pulldown assays using recombinant GST-LXRα to isolate the indicated *in vitro* translated NCOA5 constructs. Assays were performed for 2 h in the presence or absence of 2 μM T0901317. Samples were immunoblotted as indicated. Note the requirement of the NCOA5 NH_2-terminus for interacting with LXRα.

B Immunoprecipitation of Protein C-tagged LXRα from stable RAW 264.7 macrophage nuclear extracts stimulated with 1 μM T0901317 or vehicle control for 18 h, followed by immunoblotting for endogenous NCOA5 or over-expressed LXRα. Protein immunoblots of nuclear extracts are shown below.

C NCOA5 ChIP time course from primary BMMs stimulated with 1 μM T0901317 or vehicle control. qPCR was performed for the *Abca1* proximal LXRE. Note the ligand-stimulated association of NCOA5. Error bars represent ± SEM for n = 4–9 (*P = 0.02).

D NCOA5 ChIP assays from $LXR^{-/-}$ BMMs stimulated with 1 μM T0901317 or vehicle control for 18 h. qPCR was performed for the *Abca1* proximal LXRE. Error bars represent ± SEM for n = 5–6 (**P = 0.0003 for vehicle and **P = 0.002 for T0901317).

in the presence or absence of LXR ligand stimulation. Using primers spanning the proximal LXRE just upstream of the *Abca1* transcriptional start site (TSS), which is contained within the same region analyzed by PE-QMS, we detected ligand-dependent occupancy of NCOA5 on the *Abca1* promoter at 18 h (Fig 3C). We also assayed an upstream region lacking an LXRE as a negative control and failed to detect significant NCOA5 binding at 8 h or 18 h post-ligand treatment (Supplementary Fig S7B), confirming the specificity of our results. These data also indicate that despite interacting directly with LXR in the presence or absence of ligand, NCOA5 only localizes to the *Abca1* promoter *in vivo* following ligand stimulation.

To assess the requirement of LXR for NCOA5 binding at the *Abca1* promoter, we performed ChIP assays in $LXR^{-/-}$ BMMs. Notably, we detected ligand-independent occupancy of the *Abca1* promoter by NCOA5 in the absence of LXR (Fig 3D), suggesting an additional mechanism exists for NCOA5 recruitment under these conditions. Taken together, these results identify NCOA5 as an LXR corepressor, which localizes to the *Abca1* promoter *in vivo* following LXR ligand treatment to repress *Abca1* expression. In the absence of LXR, NCOA5 can still occupy the *Abca1* promoter and repress its expression through an undetermined mechanism.

NCOA5 attenuates *Abca1* expression

To investigate the dynamic role of NCOA5 as an LXR corepressor of *Abca1*, we silenced its expression in primary BMMs using shRNA and performed a time course of LXR ligand stimulation. With a non-silencing control shRNA, we observed an *Abca1* mRNA expression profile that was similar to earlier experiments (see Fig 1A), with expression peaking at 16 h post-ligand stimulation (Fig 4A). Moreover, we did not detect any significant change in *Ncoa5* expression in response to LXR ligand (Supplementary Fig S7C). Following administration of *Ncoa5* shRNA, which persistently and substantially lowered Ncoa5 expression at both the mRNA and protein levels (Supplementary Fig S7C and D), we observed a similar initial induction of *Abca1* expression (Fig 4A). However, with *Ncoa5* silencing, *Abca1* expression remained elevated even at 30 h post-ligand stimulation (Fig 4A). This effect was recapitulated at the protein level, where ABCA1 abundance was greater at 30 h post-ligand stimulation in *Ncoa5* knockdown BMMs (Fig 4B; Supplementary Fig S7E). Consistent with its proposed role as an LXR corepressor, these results demonstrate that NCOA5 is required for attenuation of *Abca1* expression following LXR ligand stimulation.

TLR3 signals to NCOA5 to suppress *Abca1* expression

The TICAM1/TRIF-dependent inflammatory receptors TLR3 and TLR4 have a profound antagonistic effect on ligand-induced LXR target gene expression (Castrillo *et al*, 2003). To investigate whether NCOA5 is involved in signal crosstalk between these pro-inflammatory TLRs and the anti-inflammatory LXR pathway, we silenced *Ncoa5* expression in primary BMMs and stimulated with LXR ligand, the TLR3 agonist polyinosinic-polycytidylic acid (PolyIC), and the TLR4 agonist bacterial lipopolysaccharide (LPS). In non-silencing shRNA controls, we detected an LXR ligand-dependent increase in *Abca1* expression at 4 h (Fig 5A and B). The addition of PolyIC or LPS, either in the presence (Fig 5A and B) or absence (Fig 5C and D) of LXR ligand, significantly reduced *Abca1* expression, together with some elevation of *Ncoa5* mRNA (Supplementary Fig S8A–D). Strikingly, knockdown of *Ncoa5* (Supplementary Fig S8A–D) abolished the ability of PolyIC but not LPS to attenuate LXR ligand-dependent *Abca1* expression (Fig 5A and B). Moreover, loss of NCOA5 failed to prevent either PolyIC- or LPS-mediated reduction of basal *Abca1* expression in the absence of LXR ligand in $LXR^{+/+}$ BMMs (Fig 5C and D).

To test the hypothesis that TLR3–LXR signal crosstalk recruits NCOA5 to the *Abca1* promoter to repress its activity, we performed NCOA5 ChIP assays in primary BMMs at 3 h post-stimulation. In macrophages lacking TLR stimulation, we failed to detect binding of NCOA5 near the proximal *Abca1* LXRE in response to LXR ligand or control (Fig 5E). However, following the addition of PolyIC to LXR ligand-stimulated BMMs, we observed a threefold increase in occupancy of the *Abca1* promoter by NCOA5 (Fig 5E). In addition, administration of PolyIC in the absence of LXR ligand failed to

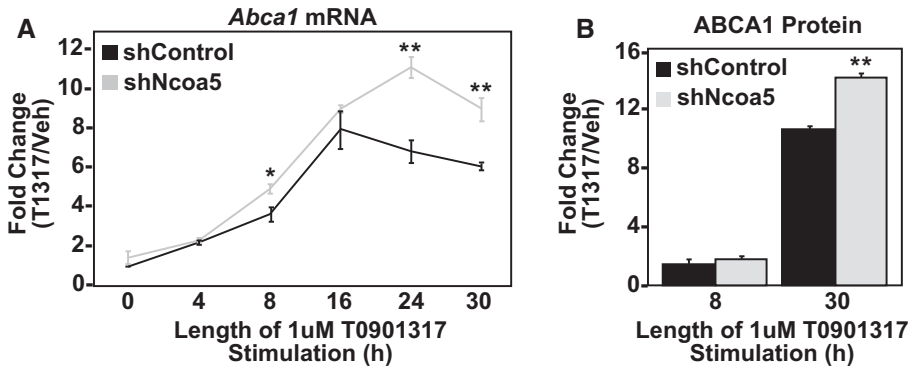

Figure 4. Attenuation of *Abca1* transcription by NCOA5.

A RT–qPCR of *Abca1* expression following 1 μM T0901317 treatment in primary BMMs infected with a non-silencing or *Ncoa5*-specific shRNA. Fold changes are shown relative to shControl 0 h. Note the elevated *Abca1* expression at 24–30 h following loss of NCOA5. Error bars represent ± SEM for n = 4–6 (**P = 0.0007 at 24 h and **P = 0.004 at 30 h, *P = 0.02).

B Quantification of ABCA1 immunoblots from primary BMMs infected as in (A). Representative immunoblot is shown in Supplementary Fig S7E. LXR ligand stimulation with 1 μM T0901317 or vehicle control was performed for 8 h or 30 h. Error bars represent ± SEM for n = 2 (**P = 0.007).

recruit NCOA5 to the *Abca1* promoter (Fig 5F). These results further indicate the responsiveness of NCOA5 to TLR3 signals only when co-stimulated with LXR ligand.

To explore the biological significance for the role of NCOA5 in mediating the TLR3-dependent repression of LXR ligand-induced *Abca1*, we performed sterol efflux assays in control and *Ncoa5* knockdown primary BMMs. In non-silencing shRNA control macrophages, we detected diminished cholesterol efflux from ABCA1 to its lipid acceptor apolipoprotein A–I (APOA1) upon addition of T0901317 and PolyIC, compared to LXR ligand alone (Fig 5G). Notably, following shRNA silencing of *Ncoa5*, LXR ligand-induced ABCA1 efflux to APOA1 failed to be impeded by TLR3 stimulation (Fig 5G). These results indicate that NCOA5 has an important role in attenuating *Abca1* expression and function in response to TLR3–LXR signal crosstalk.

To investigate the mechanism by which NCOA5 suppresses *Abca1* transcription, we examined RNA polymerase II (RNAPII) recruitment and activation. Using ChIP assays in primary BMMs, we observed increased occupancy of both unmodified/pSer5 and pSer2 RNAPII at the *Abca1* TSS in response to LXR ligand (Figs 6A and B). Notably, we detected reduced RNAPII levels when PolyIC was combined with LXR ligand (Fig 6A and B), indicating that NCOA5-mediated attenuation of *Abca1* expression in response to TLR3–LXR signal crosstalk correlates with a defect in RNAPII function, likely through recruitment.

To ascertain the role of LXR in this RNAPII defect, we performed the above experiments in $LXR^{-/-}$ BMMs. We did not detect an LXR ligand-dependent increase in occupancy of either unmodified/pSer5 or pSer2 RNAPII at the *Abca1* TSS (Fig 6C and D). However, we still observed a reduction in RNAPII occupancy following treatment

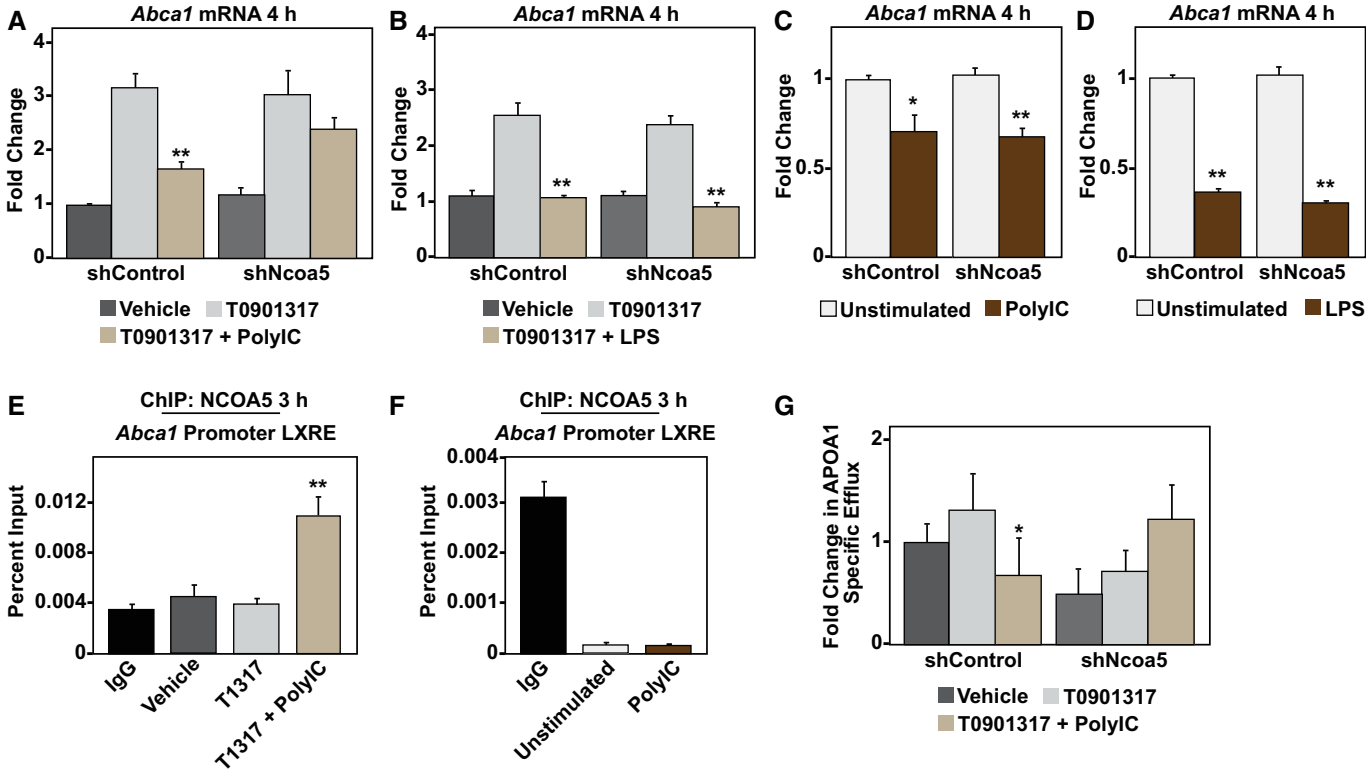

Figure 5. NCOA5 mediates TLR3–LXR signal crosstalk by antagonizing *Abca1* expression and function.

A, B RT–qPCR of *Abca1* expression from primary BMMs infected with non-silencing or *Ncoa5*-specific shRNAs. Ligand stimulations were performed for 4 h with vehicle control, 1 μM T0901317 alone or together with 6 μg/ml PolyIC (A) or 10 ng/ml LPS (B). Fold changes are shown relative to vehicle-stimulated shControl. Note only the loss of TLR3-mediated repression following *Ncoa5* silencing. Error bars represent ± SEM for n = 4–10 (**P = 0.0003 for A, **P = 0.0004 for shControl in B, **P = 0.0002 for shNcoa5 in B versus T0901317).

C, D RT–qPCR of *Abca1* expression from primary BMMs infected with non-silencing or *Ncoa5*-specific shRNAs. Ligand stimulations were performed for 4 h unstimulated, or with 6 μg/ml PolyIC (C) or 10 ng/ml LPS (D). Fold changes are shown relative to unstimulated shControl. Error bars represent ± SEM for n = 4–6 (**P = 0.0006 for C, **P = 0.00000001 for shControl in D, **P = 0.000001 for shNcoa5 in D, *P = 0.013 versus T0901317).

E NCOA5 ChIP assays from primary BMMs stimulated for 3 h with 1 μM T0901317, 1 μM T0901317 + 6 μg/ml PolyIC, or vehicle control. qPCR was performed for the *Abca1* proximal LXRE. Note the increased occupancy only in the presence of both lipid and inflammatory ligands. Error bars represent ± SEM for n = 8–12 (**P = 0.0007 versus T0901317).

F NCOA5 ChIP assays from primary BMMs stimulated for 3 h with 6 μg/ml PolyIC or left unstimulated. qPCR was performed for the *Abca1* proximal LXRE. Error bars represent ± SEM for n = 5–6.

G Cholesterol efflux assays to APOA1 from primary BMMs infected with non-silencing or *Ncoa5*-specific shRNAs. Agonist stimulations were performed for 6 h. Error bars represent ± SEM for n = 3 (*P = 0.02 versus T0901317).

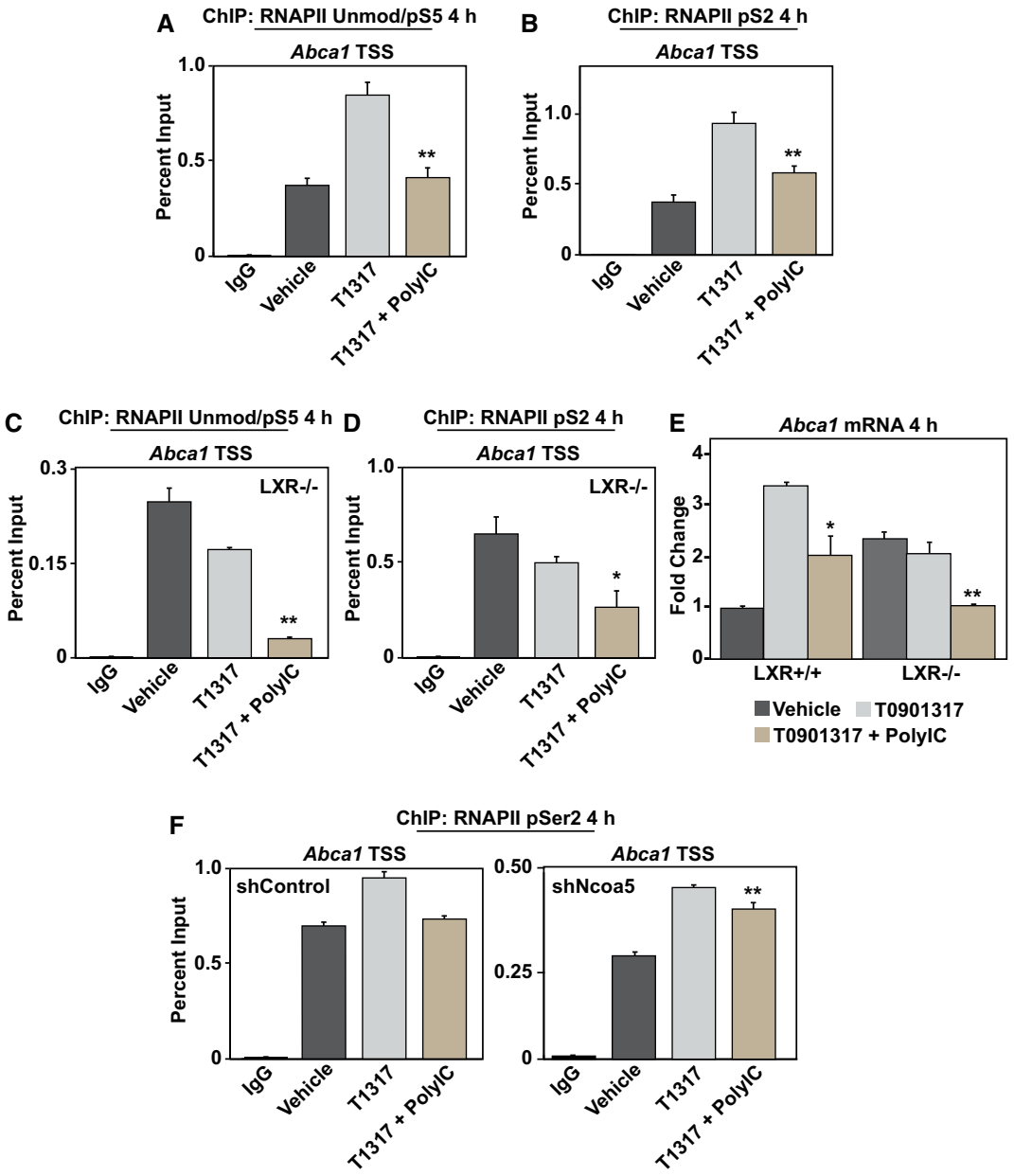

Figure 6. NCOA5 represses *Abca1* expression following TLR3–LXR signal crosstalk by inhibiting RNAPII function.

A, B Unmodified/pSer5 RNAPII (A) or RNAPII pSer2 (B) ChIP assays from primary BMMs stimulated for 4 h with 1 μM T0901317, 1 μM T0901317 + 6 μg/ml PolyIC, or vehicle control. qPCR was performed for the *Abca1* TSS. Error bars represent ± SEM for $n = 6$–9 (**$P = 0.0001$ in A, **$P = 0.002$ in B versus T0901317).

C, D RNAPII ChIP assays as in (A, B) but performed from $LXR^{-/-}$ BMMs. Error bars represent ± SEM for $n = 5$–9 (**$P = 0.000000001$, *$P = 0.02$ versus T0901317).

E RT–qPCR of *Abca1* expression from $LXR^{+/+}$ versus $LXR^{-/-}$ BMMs. Ligand stimulations were performed for 4 h with vehicle control, 1 μM T0901317, or 1 μM T0901317 together with 6 μg/ml PolyIC. Fold changes are shown relative to vehicle-stimulated $LXR^{+/+}$. Error bars represent ± SEM for $n = 4$ (**$P = 0.004$, *$P = 0.012$ versus T0901317).

F RNAPII pSer2 ChIP assays from primary BMMs infected with non-silencing or *Ncoa5*-specific shRNAs. Ligand stimulations were performed for 4 h with vehicle control, 1 μM T0901317, or 1 μM T0901317 + 6 μg/ml PolyIC. qPCR was performed for the *Abca1* TSS. Note RNAPII pSer2 returns to baseline occupancy following TLR3 stimulation in shControl but not shNcoa5 BMMs (**$P = 0.004$ versus baseline). Error bars represent ± SEM for $n = 3$ from 11 mice.

with T0901317 and PolyIC (Fig 6C and D). In support of this, we also detected decreased *Abca1* mRNA expression in response to both treatments in $LXR^{-/-}$ BMMs (Fig 6E; Supplementary Fig S8E), further suggesting that NCOA5 can function even in the absence of LXR.

To determine whether TLR3–LXR signal crosstalk prevents RNAPII function through NCOA5, we performed ChIP assays following silencing of *Ncoa5* expression. With a non-silencing control, we observed increased RNAPII pSer2 occupancy at the *Abca1* TSS in response to LXR ligand (Fig 6F). The addition of both LXR and TLR3

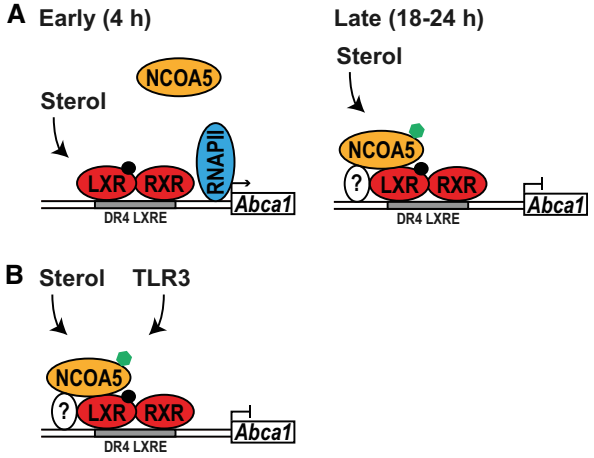

Figure 7. Model for the NCOA5-mediated repression of *Abca1* expression.

A In response to sterol ligand treatment, LXR–RXR heterodimers initially induce the transcription of *Abca1* through recruitment and activation of RNAPII (left). Following prolonged sterol ligand treatment, the NCOA5 repressor directly interacts with LXR at the *Abca1* promoter. This repressor complex inhibits the recruitment and function of RNAPII resulting in attenuated expression of *Abca1* (right). We hypothesize that prolonged sterol ligand treatment induces a regulatory modification on NCOA5 (shown in green), such as phosphorylation, which facilitates its recruitment to LXR.

B Crosstalk between pro-inflammatory TLR3 and anti-inflammatory LXR pathways promotes the association of NCOA5 with LXR, resulting in the inhibition of RNAPII recruitment and function, and repression of *Abca1* gene expression. The regulatory modification of NCOA5 following activation of these two pathways may be similar or distinct to that in (A). We also cannot discount the contribution of additional constituents of this transcriptional complex to the recruitment of NCOA5.

ligands returned RNAPII pSer2 occupancy to basal levels ($P = 0.33$ versus Veh; Fig 6F). Following *Ncoa5* gene silencing, RNAPII pSer2 binding remained elevated, failing to return to basal levels, in response to both LXR and TLR3 ligands ($P = 0.004$ versus Veh; Fig 6F). Taken together, these data establish NCOA5 as a critical downstream mediator of the crosstalk between the pro-inflammatory TLR3 and anti-inflammatory LXR pathways, and in response to these signals, NCOA5 represses macrophage cholesterol efflux through inhibition of RNAPII function at the *Abca1* gene locus (Fig 7).

Discussion

Inappropriate and sustained signaling events interfere with homeostasis by perturbing regulatory network function, resulting in chronic disease. In atherosclerosis, these signals arise from chronic inflammation and inhibit the macrophage homeostatic response to hyperlipidemia, specifically the cholesterol efflux pathway, which results in foam cell formation and plaque progression. While LXRs directly induce transcription of the transporters responsible for cholesterol efflux, it currently remains unknown whether additional transcriptional regulatory proteins are recruited to these promoters by inflammatory signals to block LXR-dependent gene regulation, and the mechanisms by which this might occur.

We hypothesized that LXR cofactors receive these inflammatory signals from TLRs to directly modulate lipid-mediated gene expression. We therefore characterized the occupancy of the *Abca1* promoter by transcriptional regulators using promoter enrichment-quantitative mass spectrometry (PE-QMS). Notably, PE-QMS provides a DNA-context-dependent method of identifying transcriptional regulatory complexes that requires no *a priori* knowledge of transcription factor identity (Ranish *et al*, 2003, 2004). Moreover, it can identify cofactor and combinatorial interactions, which are not readily achieved using epigenomic and chromatin accessibility information (Ramsey *et al*, 2010; Neph *et al*, 2012; Sherwood *et al*, 2014). A unique aspect of our PE-QMS design was assessing not only the effect of LXR ligand stimulation on gene regulatory complex composition, but also the subset of that response which was dependent on LXR promoter binding. Identification of these subsets would otherwise be unattainable using protein-, informatics-, or omics-based methods.

We identified five previously unknown LXR-dependent regulators of *Abca1* and demonstrated that four of these proteins control *Abca1* expression in response to LXR ligand stimulation. We have established for the first time, to our knowledge, that NCOA5 functions as an LXR corepressor to attenuate *Abca1* expression. In our PE-QMS experiments, NCOA5 binding was twofold lower but not undetectable in the absence of LXR ligand stimulation. This may explain the reduction in *Abca1*-luciferase expression by NCOA5 even in the absence of ligand (Fig 2C). Notably, our primary BMM ChIP and expression analyses indicate a ligand-dependent NCOA5 occupancy and function at the *Abca1* locus when LXR is present.

TLRs recognizing endogenous ligands transmit inflammatory signals in atherosclerosis; however, their role is complicated by their expression and function in multiple cell types. TLR2 functions in endothelial cells to recruit monocytes/macrophages to plaques to facilitate inflammation (Mullick *et al*, 2005, 2008; Monaco *et al*, 2009). TLR4 also promotes inflammation leading to atherosclerosis, albeit through a macrophage centric mechanism (Xu *et al*, 2001; Michelsen *et al*, 2004; Stewart *et al*, 2010).

Recent studies have also identified a role for TLR3 signaling in promoting atherosclerosis (Zimmer *et al*, 2011). TLR3 can sense RNA released from necrotic cells as a result of the inflammatory process (Kariko *et al*, 2004; Cavassani *et al*, 2008; Ahmad *et al*, 2010; Baiersdorfer *et al*, 2010). Loss of TICAM1/TRIF function, the downstream adaptor for TLR3, either systemically or specific to the hematopoietic system, alleviates inflammation and reduces atherosclerosis (Lundberg *et al*, 2013; Richards *et al*, 2013). Moreover, bone marrow-specific deletion of *Tlr3* produces a similar phenotype (Lundberg *et al*, 2013), suggesting that the macrophage TLR3 signaling pathway could be an important mediator of inflammation in atherosclerosis. Conversely, global *Tlr3* deletion exacerbates lesion size, indicating an additional role for non-bone marrow-derived cells in atherosclerosis (Cole *et al*, 2011; Richards *et al*, 2013).

Signal crosstalk between the pro-inflammatory TLR3 and anti-inflammatory LXR pathways has previously been reported to induce IRF3 expression, which competes with LXR for the coactivator EP300, resulting in reduced *Abca1* transcription (Castrillo *et al*, 2003). Our results demonstrate that in addition to competition for a shared coactivator, TLR3–LXR signal crosstalk actively recruits the

corepressor NCOA5 to an LXR-regulated promoter to repress *Abca1* gene expression.

Notably, the repression of *Abca1* following PolyIC treatment alone is independent of NCOA5. Moreover, LPS-mediated repression of *Abca1* is completely independent of NCOA5. One possible explanation for this is a regulatory event, such as a post-translational modification of NCOA5, which specifically occurs when both the TLR3 and LXR pathways, but not the TLR4 and LXR pathways, are simultaneously activated (Fig 7). TLR4 induction results in widespread phosphoproteome changes (Weintz *et al*, 2010), so it is reasonable to hypothesize that phosphoproteome changes would occur downstream of TLR3. Alternatively, there could be distinct but complementary events mediated by the TLR3 and LXR pathways that target NCOA5 function. For instance, activation of TLR3 signaling could result in modification of NCOA5, while ligand binding to LXR could permit binding of modified NCOA5 to LXR. Castrillo *et al* (2003) observed the reduction in *Abca1* expression by these signals was independent of IFNαβ, which may further restrict potential candidates. Future quantitative mass spectrometry studies will be critical in delineating these mechanisms.

We also discovered that NCOA5 binds the *Abca1* promoter and retains a repressive function in the absence of LXR. An intriguing hypothesis is these proteins are part of a larger transcriptional complex and that NCOA5 might associate with LXR and another constituent. This additional interaction would be sufficient to recruit NCOA5 in the absence of LXR, such as in $LXR^{-/-}$ BMMs. Future experiments will focus on identifying this factor, using our list of candidate regulatory proteins identified by PE-QMS.

Several LXR cofactors reported to modulate its activity also regulate chromatin structure, including p300, SMARCA4, NCOA6, and the NCOR complex (Castrillo *et al*, 2003; Wagner *et al*, 2003; Huuskonen *et al*, 2004, 2005; Lee *et al*, 2008; Jakobsson *et al*, 2009). We detected LXR ligand-stimulated binding of the chromatin regulators SMARCC2, INO80, and HIRA to the *Abca1* promoter by PE-QMS (Fig 1C). Despite the fact we targeted a region of the *Abca1* locus devoid of nucleosomes for PE-QMS, nucleosomes are present adjacent to this region (Supplementary Fig S2), suggesting the binding of SMARCC2, INO80, and HIRA may be important for remodeling these regions or perhaps for long-distance interactions. However, we cannot discount the possibility of a non-chromatin-related role for these proteins, such as that described for the NCOR complex component HDAC3 (Sun *et al*, 2013).

PE-QMS is not without its limitations. Chromatin structure is an important regulator of gene expression and can affect transcription factor binding. We controlled for this by using an open chromatin region, as well as confirming NCOA5 genome localization by ChIP. However, recent studies are beginning to show the feasibility of capturing and identifying chromatin-associated proteins in their native context (Dejardin & Kingston, 2009; Pourfarzad *et al*, 2013; Alabert *et al*, 2014), and it will be attractive to apply these approaches to the analysis of low copy number, dynamic, chromatin-associated complexes in the future.

Another limitation of this study is we cannot be completely certain the full compendium of proteins bound to the *Abca1* promoter was identified. For instance, MED15 is part of the large multi-subunit Mediator complex. The lack of detection of other subunits in this complex may reflect their instability on this promoter under our experimental conditions, or duty cycle limitations of the data-dependent mass spectrometry strategy employed. Another recent study using a similar enrichment strategy identified four Mediator subunits bound to their promoter sequences (Foulds *et al*, 2013). Recent advances in mass spectrometry-based protein identification technologies with improved sensitivity and reproducibility, such as targeted (Mirzaei *et al*, 2013) and data-independent peptide identification approaches (Gillet *et al*, 2012; Egertson *et al*, 2013; Lambert *et al*, 2013), hold great promise for overcoming these limitations and are currently being explored.

Whether aberrant targeting of NCOA5 to the *Abca1* promoter to repress its expression exacerbates disease progression remains an important question with therapeutic relevance. Impairment of cholesterol efflux *in vivo* promotes foam cell formation and enhances atherosclerosis (van Eck *et al*, 2002; Tangirala *et al*, 2002; Yvan-Charvet *et al*, 2007). Moreover, macrophages display an enhanced inflammatory response to TLR signals in the absence of cholesterol transporter gene expression (van Eck *et al*, 2002; Yvan-Charvet *et al*, 2008; Zhu *et al*, 2008). Taken together, this suggests that NCOA5 activity could potentiate the chronic inflammatory process responsible for atherosclerosis.

Materials and Methods

Macrophage isolation and cell culture

All experiments were performed in accordance with the Institute for Systems Biology and Seattle Biomedical Research Institute Institutional Animal Care and Use Committees. Mice were euthanized by CO_2 asphyxiation. C57BL6, *Nr1h3*$^{-/-}$, *Nr1h2*$^{-/-}$ mice were obtained from The Jackson Laboratory, and the latter two strains were crossed in house to generate $LXR^{-/-}$ double knockouts. BMMs were isolated from 8- to 12-week-old females as previously described (Gilchrist *et al*, 2006). Bone marrow was collected from femurs with complete RPMI 1640 media (10% FBS, 100 U/ml penicillin and streptomycin, 2 mM L-glutamine) (Corning Cellgro; Life Technologies) supplemented with 50 ng/ml recombinant human macrophage colony-stimulating factor (rhM-CSF; Peprotech). Collected bone marrow was grown on non-tissue culture-treated dishes for 6 days, then plated on tissue culture dishes, and stimulated with T0901317 (CAS 293754-55-9; Cayman Chemical), PolyIC (6 μg/ml; GE Healthcare), and/or LPS (10 ng/ml; *Salmonella minnesota*; List Biologicals) such that BMMs were harvested on day 7. All ligands were administered simultaneously for combined treatments. RAW 264.7 macrophages (ATCC TIB-71) and Phoenix cells (Kinsella & Nolan, 1996) were cultured in complete RPMI without rhM-CSF. Cell lines were tested for the absence of mycoplasma contamination.

Promoter enrichment-quantitative mass spectrometry (PE-QMS)

A promoter region of *Abca1* (chr4:53,172,714-53,173,035; NCBI Build 37; mm9) was used to enrich for associated gene regulatory complexes from RAW 264.7 macrophage nuclear extracts (Dignam *et al*, 1983). The promoter region was PCR amplified with a biotinylated forward primer and bound to NeutrAvidin–agarose beads. Following blocking, immobilized promoters were incubated with nuclear extracts in 20 mM Hepes, pH 7.4, 10% glycerol,

60 mM NaCl, 1 mM EDTA, 5 mM $MgCl_2$, 2 mM DTT, and 0.05% NP-40 for 2 h. Promoter–protein complexes were washed three times with the above buffer and then twice with the above buffer lacking NP-40 and then eluted twice with 15 mM Tris, pH 8.3, 600 mM NaCl, 5.5 M urea, and 1 mM EDTA for 30 min at 37°C each. Eluted proteins were digested with trypsin and purified using C18 reversed-phase chromatography. Orthogonal label-free and isotope labeling strategies were separately employed for protein quantification. Labeled peptides were subsequently fractionated by Partisphere strong cation exchange chromatography. Purified peptides were separated by online reversed-phase HPLC over an increasing gradient of acetonitrile and analyzed by mass spectrometry (LTQ-Orbitrap Velos and LTQ-Orbitrap XL). Raw output files were processed with GeneData Expressionist and Mascot (label free) or the Trans-Proteomic Pipeline and X!Tandem (labeled). A reverse sequence database was used to assess FDR. Data were manually inspected to ensure accuracy of identifications and quantifications. Data were filtered to remove single peptide identifications, along with proteins not satisfying a 1% FDR cutoff. In addition, proteins corresponding to genes not expressed in primary BMMs were removed (Ramsey *et al*, 2008; Gold *et al*, 2012). Using correlated quantitative information, we identified 79 promoter-associated proteins in the ligand-stimulated experiments. We used a 1.5-fold cutoff as described in the Results to subdivide proteins by their ligand dependency and their LXR dependency. A detailed description of this methodology is available in the Supplementary Materials and Methods.

GO enrichment and network analysis

GO enrichment analysis was performed using DAVID ($P < 0.01$) (Huang da *et al*, 2009). All expressed transcripts from unstimulated mouse primary BMMs (Ramsey *et al*, 2008; Gold *et al*, 2012) were used as background to calculate enrichment. Protein–protein network analysis was performed using ingenuity pathway analysis (Ingenuity) and GeneMANIA (Mostafavi *et al*, 2008), filtering for only physical associations. The network was filtered to include only LXR-dependent regulators and their associations with the immune system.

Quantitative RT–PCR

Total RNA was isolated using TRIzol Reagent (Life Technologies) according to manufacturers' protocol. RNA was reverse transcribed using random primers and Superscript II (Life Technologies) according to manufacturers' protocol. cDNA was analyzed by real-time PCR using Taqman Gene Expression assays (Life Technologies) (Supplementary Table S3). Data were acquired using a 7900HT Fast Real-Time PCR System (Life Technologies) and were normalized to *Eef1a1* transcript expression within individual samples.

Reporter assays

Abca1-luciferase was constructed by amplifying the 53,173,035–53,172,714 regulatory sequence (same sequence used for PE-QMS) from mouse gDNA and cloning it into pGL3-basic (Promega). Ncoa5-ΔNT was designed by removing the NH_2-terminal 840 nt from the full-length cDNA (Thermo Scientific). RAW 264.7 macrophages were transfected using Lipofectamine 2000 (Life Technologies) according to manufacturers' protocol. Cells were lysed with 1× passive lysis buffer, and luciferase assays were analyzed on a GloMax 96 Microplate Luminometer (Promega). All luciferase activity was normalized to co-transfected *Renilla* luciferase and to the pGL3-basic empty reporter construct.

Chromatin immunoprecipitation (ChIP) assays

1.5×10^7 BMMs were crosslinked with 1% formaldehyde in PBS for 10 min at room temperature, quenched with 125 mM glycine for 5 min at room temperature, and then washed 3× with ice cold PBS. Cells were scraped, pelleted, and lysed in RIPA buffer (10 mM Tris, pH 7.4, 140 mM NaCl, 0.1% SDS, 1% Triton X-100, 1% Na-deoxycholate). Extracts were sonicated 5 × 1 min using an Ultrasonic Processor 130 W at 3 W and 35% output. NCOA5 (A300-790A; Bethyl Laboratories), RNAPII unmodified/pSer5 (05-623; Millipore), RNAPII pSer2 (ab5095; Abcam), rabbit IgG (sc2027; Santa Cruz Biotechnology), or mouse IgG antibodies (sc2025; Santa Cruz Biotechnology) were pre-conjugated to Protein G Dynabeads (Life Technologies) in 0.5% BSA in PBS and used to immunoprecipitate sheared chromatin complexes overnight. Complexes were washed twice with Wash Buffer I (20 mM Tris, pH 7.4, 150 mM NaCl, 0.1% SDS, 1% Triton X-100, 2 mM EDTA), once with Wash Buffer II (10 mM Tris, pH 7.4, 250 mM LiCl, 0.5% NP-40, 0.5% Na-deoxycholate, 1 mM EDTA), and once with TE (10 mM Tris, pH 8.0, 1 mM EDTA) or washed three times with RIPA buffer and once with TE. Complexes were eluted twice with 1% SDS in TE at 65°C for 15 min, and eluates were combined. Protein was digested, and crosslinks reversed (40 mM Tris, pH 8.0, 10 mM EDTA, 240 mM NaCl, 25 μg Proteinase K) at 55°C for 2.5 h and then 65°C overnight. DNA was PCR-purified (Qiagen) prior to qPCR analysis using SYBR Green (Life Technologies) (Supplementary Table S3).

Pulldowns, immunoprecipitation, and immunoblots

Recombinant GST and GST-LXRα proteins were expressed from the pGEX4T vector (GE Healthcare) and purified from isopropyl-β-D-thiogalactoside (IPTG; 2 mM)-induced *E. coli* BL21(DE3)pLysS using glutathione-Sepharose beads (GE Healthcare). Full-length and mutant *Ncoa5* cDNAs were generated by PCR, cloned into pEF6-V5-His (Life Technologies), and transcribed/translated *in vitro* using the TNT T7 Quick Coupled System (Promega) according to manufacturer's protocol. *In vitro* translated proteins (5 μl) were then incubated with 2.5 μg GST proteins pre-bound to glutathione-Sepharose beads for 2 h at 4°C. Beads were washed 3× with NETN Buffer (50 mM Tris, pH 8.0, 100 mM NaCl, 0.1% NP-40, 1 mM EDTA) and boiled in LDS Sample Buffer (Life Technologies) to elute complexes prior to Western blot analysis. For IPs, RAW 264.7 macrophages stably expressing Protein C-tagged LXRα were maintained in complete RPMI plus 10 μg/ml blasticidin. The Protein C tag construct was generated and kindly provided by Adrian Ozinsky. Co-IPs were performed from nuclear extracts. Due to the Protein C tag, EDTA was omitted from all buffers except elution buffer. Protein C-agarose affinity matrix (Clone HPC4; Roche Applied Science) was used for IPs. Protein was eluted using 5 mM EDTA and analyzed by Western blotting. Antibodies used for Western

immunoblotting were NCOA5 (A300-790A; Bethyl Laboratories), LXR (sc1000; Santa Cruz Biotechnology), ABCA1 (ab18180; Abcam), V5-Tag (MCA1360; AbD Serotec), and tubulin (Clone DM1A; Sigma-Aldrich). Blots were imaged using a CCD camera (FluorChem E; Protein Simple) and quantified using AlphaView SA software.

Retroviral infections

miR-30-based shRNAs were designed as described (Paddison *et al*, 2004), based on siRNA sequences from Thermo Scientific, and cloned into the LMP retroviral vector (Dickins *et al*, 2005) (Supplementary Table S3). A non-silencing negative control sequence was used to ensure specificity (Thermo Scientific). Retrovirus was prepared by transfecting the Phoenix Ecotropic packaging cell line (Kinsella & Nolan, 1996) with the above constructs using Lipofectamine 2000 (Life Technologies). After 48 h, viral supernatant was removed, 0.44 μm filtered, and used to infect day 2 BMMs. Infections were supplemented with 6 μg/ml polybrene (Millipore) and 50 ng/ml rhM-CSF and performed for 2 h at 1,800 rpm at 32°C, then for another 2 h at 37°C. Viral media were replaced with complete RPMI media for another 72 h, and then, infected cells were selected with 5 μg/ml puromycin (Invivogen) for 5 days. For overexpression studies, *Ncoa5* cDNA was cloned into the LMP retroviral vector and infections were performed in day 4 BMMs as indicated above. Infected cells were harvested on day 7.

Cholesterol efflux assays

Macrophages were labeled with 1 μCi/ml [1,2,^{3}H(N)]-cholesterol (Perkin Elmer) in RPMI containing 0.2% BSA, 50 ng/ml MCSF, 5 μg/ml puromycin, and 2 μg/ml acyl-coenzyme A cholesterol acyltransferase (ACAT) inhibitor (Sandoz 58-035; Sigma) for 24 h. Macrophages were washed and equilibrated in RPMI containing 0.2% BSA, 5 μg/ml puromycin, and 2 μg/ml ACAT inhibitor for 6 h. Stimulations with vehicle, 1 μM T0901317, or 1 μM T0901317 + 6 μg/ml PolyIC were performed simultaneously with equilibration. Efflux was measured following wash and incubation for 4 h with equilibration media containing 10 μg/ml mouse APOA1 protein (IgG Fc tagged; Life Technologies) or IgG protein (Meridian Life Science) as a control. Supernatants were clarified by centrifugation, and one-fifth measured by liquid scintillation counting. Cells were lysed in 0.1 N NaOH + 0.2% SDS and 1/20 measured by liquid scintillation counting. After adjusting for dilutions, percent efflux was calculated by dividing the ^{3}H-cholesterol effluxed to the media by the total ^{3}H-cholesterol present in the cells and media. Specific efflux to APOA1 was calculated in response to each agonist by subtracting out any background efflux to IgG.

Statistical analysis

All error bars are presented as standard error of the means. Statistical significance of means was calculated using the two-tailed Student's *t*-test, using a cutoff of $P < 0.05$. The one exception to this was the GO enrichment analysis, where we used a cutoff of $P < 0.01$ in a modified version of the Fisher's exact test called the EASE score (Huang da *et al*, 2009).

Raw data deposition

All raw proteomics data were deposited in Peptide Atlas under the identifiers PASS00515, PASS00516, and PASS00517.

Supplementary information for this article is available online: http://emboj.embopress.org

Acknowledgements

We thank Peter Askovich and David Shteynberg for helpful assistance with mass spectrometry analysis software, Jay Heinecke and Angela Irwin for helpful assistance with the sterol efflux protocol, and Alan Diercks for critical reading of the manuscript. Research reported in this publication was supported by the Canadian Institutes of Health Research Fellowship MFE-112984 (to M.A.G.), the National Heart, Lung, and Blood Institute Award Number HL098807 (to S.A.R.), the National Institute of Allergy and Infectious Diseases Award Numbers R01 AI032972, R01 AI025032, and U19 AI100627 (to A.A.), and the National Institute of General Medical Sciences Center for Systems Biology Award Number 2P50 GM076547 (J.A.R.).

Author contributions

MAG designed, performed, and analyzed experiments; SAR performed network analysis; IP assisted with shRNA experiments; AA and JAR supervised the studies; and MAG, ESG, AA, and JAR conceived experiments and wrote the manuscript.

Conflict of interest

The authors declare that they have no conflict of interest.

References

Ahmad U, Ali R, Lebastchi AH, Qin L, Lo SF, Yakimov AO, Khan SF, Choy JC, Geirsson A, Pober JS, Tellides G (2010) IFN-gamma primes intact human coronary arteries and cultured coronary smooth muscle cells to double-stranded RNA- and self-RNA-induced inflammatory responses by upregulating TLR3 and melanoma differentiation-associated gene 5. *J Immunol* 185: 1283 – 1294

Aiello RJ, Brees D, Bourassa PA, Royer L, Lindsey S, Coskran T, Haghpassand M, Francone OL (2002) Increased atherosclerosis in hyperlipidemic mice with inactivation of ABCA1 in macrophages. *Arterioscler Thromb Vasc Biol* 22: 630 – 637

Alabert C, Bukowski-Wills JC, Lee SB, Kustatscher G, Nakamura K, de Lima AF, Menard P, Mejlvang J, Rappsilber J, Groth A (2014) Nascent chromatin capture proteomics determines chromatin dynamics during DNA replication and identifies unknown fork components. *Nat Cell Biol* 16: 281 – 293

Ashburner M, Ball CA, Blake JA, Botstein D, Butler H, Cherry JM, Davis AP, Dolinski K, Dwight SS, Eppig JT, Harris MA, Hill DP, Issel-Tarver L, Kasarskis A, Lewis S, Matese JC, Richardson JE, Ringwald M, Rubin GM, Sherlock G (2000) Gene ontology: tool for the unification of biology. The Gene Ontology Consortium. *Nat Genet* 25: 25 – 29

Baiersdorfer M, Schwarz M, Seehafer K, Lehmann C, Heit A, Wagner H, Kirschning CJ, Koch-Brandt C (2010) Toll-like receptor 3 mediates expression of clusterin/apolipoprotein J in vascular smooth muscle cells stimulated with RNA released from necrotic cells. *Exp Cell Res* 316: 3489 – 3500

Bento JL, Palmer ND, Zhong M, Roh B, Lewis JP, Wing MR, Pandya H, Freedman BI, Langefeld CD, Rich SS, Bowden DW, Mychaleckyj JC (2008)

Heterogeneity in gene loci associated with type 2 diabetes on human chromosome 20q13.1. *Genomics* 92: 226 – 234

Bodzioch M, Orso E, Klucken J, Langmann T, Bottcher A, Diederich W, Drobnik W, Barlage S, Buchler C, Porsch-Ozcurumez M, Kaminski WE, Hahmann HW, Oette K, Rothe G, Aslanidis C, Lackner KJ, Schmitz G (1999) The gene encoding ATP-binding cassette transporter 1 is mutated in Tangier disease. *Nat Genet* 22: 347 – 351

Brooks-Wilson A, Marcil M, Clee SM, Zhang LH, Roomp K, van Dam M, Yu L, Brewer C, Collins JA, Molhuizen HO, Loubser O, Ouelette BF, Fichter K, Ashbourne-Excoffon KJ, Sensen CW, Scherer S, Mott S, Denis M, Martindale D, Frohlich J *et al* (1999) Mutations in ABC1 in Tangier disease and familial high-density lipoprotein deficiency. *Nat Genet* 22: 336 – 345

Calkin AC, Tontonoz P (2012) Transcriptional integration of metabolism by the nuclear sterol-activated receptors LXR and FXR. *Nat Rev Mol Cell Biol* 13: 213 – 224

Castrillo A, Joseph SB, Vaidya SA, Haberland M, Fogelman AM, Cheng G, Tontonoz P (2003) Crosstalk between LXR and toll-like receptor signaling mediates bacterial and viral antagonism of cholesterol metabolism. *Mol Cell* 12: 805 – 816

Cavassani KA, Ishii M, Wen H, Schaller MA, Lincoln PM, Lukacs NW, Hogaboam CM, Kunkel SL (2008) TLR3 is an endogenous sensor of tissue necrosis during acute inflammatory events. *J Exp Med* 205: 2609 – 2621

Cole JE, Navin TJ, Cross AJ, Goddard ME, Alexopoulou L, Mitra AT, Davies AH, Flavell RA, Feldmann M, Monaco C (2011) Unexpected protective role for Toll-like receptor 3 in the arterial wall. *Proc Natl Acad Sci USA* 108: 2372 – 2377

Costet P, Luo Y, Wang N, Tall AR (2000) Sterol-dependent transactivation of the ABC1 promoter by the liver X receptor/retinoid X receptor. *J Biol Chem* 275: 28240 – 28245

Dejardin J, Kingston RE (2009) Purification of proteins associated with specific genomic Loci. *Cell* 136: 175 – 186

Dickins RA, Hemann MT, Zilfou JT, Simpson DR, Ibarra I, Hannon GJ, Lowe SW (2005) Probing tumor phenotypes using stable and regulated synthetic microRNA precursors. *Nat Genet* 37: 1289 – 1295

Dignam JD, Lebovitz RM, Roeder RG (1983) Accurate transcription initiation by RNA polymerase II in a soluble extract from isolated mammalian nuclei. *Nucleic Acids Res* 11: 1475 – 1489

van Eck M, Bos IS, Kaminski WE, Orso E, Rothe G, Twisk J, Bottcher A, Van Amersfoort ES, Christiansen-Weber TA, Fung-Leung WP, Van Berkel TJ, Schmitz G (2002) Leukocyte ABCA1 controls susceptibility to atherosclerosis and macrophage recruitment into tissues. *Proc Natl Acad Sci USA* 99: 6298 – 6303

Egertson JD, Kuehn A, Merrihew GE, Bateman NW, MacLean BX, Ting YS, Canterbury JD, Marsh DM, Kellmann M, Zabrouskov V, Wu CC, MacCoss MJ (2013) Multiplexed MS/MS for improved data-independent acquisition. *Nat Methods* 10: 744 – 746

Foulds CE, Feng Q, Ding C, Bailey S, Hunsaker TL, Malovannaya A, Hamilton RA, Gates LA, Zhang Z, Li C, Chan D, Bajaj A, Callaway CG, Edwards DP, Lonard DM, Tsai SY, Tsai MJ, Qin J, O'Malley BW (2013) Proteomic analysis of coregulators bound to ERalpha on DNA and nucleosomes reveals coregulator dynamics. *Mol Cell* 51: 185 – 199

Gao S, Li A, Liu F, Chen F, Williams M, Zhang C, Kelley Z, Wu CL, Luo R, Xiao H (2013) NCOA5 haploinsufficiency results in glucose intolerance and subsequent hepatocellular carcinoma. *Cancer Cell* 24: 725 – 737

Ghisletti S, Huang W, Ogawa S, Pascual G, Lin ME, Willson TM, Rosenfeld MG, Glass CK (2007) Parallel SUMOylation-dependent pathways mediate gene- and signal-specific transrepression by LXRs and PPARgamma. *Mol Cell* 25: 57 – 70

Gilchrist M, Thorsson V, Li B, Rust AG, Korb M, Roach JC, Kennedy K, Hai T, Bolouri H, Aderem A (2006) Systems biology approaches identify ATF3 as a negative regulator of Toll-like receptor 4. *Nature* 441: 173 – 178

Gillet LC, Navarro P, Tate S, Rost H, Selevsek N, Reiter L, Bonner R, Aebersold R (2012) Targeted data extraction of the MS/MS spectra generated by data-independent acquisition: a new concept for consistent and accurate proteome analysis. *Mol Cell Proteomics* 11: O111.016717

Gold ES, Ramsey SA, Sartain MJ, Selinummi J, Podolsky I, Rodriguez DJ, Moritz RL, Aderem A (2012) ATF3 protects against atherosclerosis by suppressing 25-hydroxycholesterol-induced lipid body formation. *J Exp Med* 209: 807 – 817

Huang W, Ghisletti S, Saijo K, Gandhi M, Aouadi M, Tesz GJ, Zhang DX, Yao J, Czech MP, Goode BL, Rosenfeld MG, Glass CK (2011) Coronin 2A mediates actin-dependent de-repression of inflammatory response genes. *Nature* 470: 414 – 418

Huang da W, Sherman BT, Lempicki RA (2009) Systematic and integrative analysis of large gene lists using DAVID bioinformatics resources. *Nat Protoc* 4: 44 – 57

Huuskonen J, Fielding PE, Fielding CJ (2004) Role of p160 coactivator complex in the activation of liver X receptor. *Arterioscler Thromb Vasc Biol* 24: 703 – 708

Huuskonen J, Vishnu M, Fielding PE, Fielding CJ (2005) Activation of ATP-binding cassette transporter A1 transcription by chromatin remodeling complex. *Arterioscler Thromb Vasc Biol* 25: 1180 – 1185

Jakobsson T, Venteclef N, Toresson G, Damdimopoulos AE, Ehrlund A, Lou X, Sanyal S, Steffensen KR, Gustafsson JA, Treuter E (2009) GPS2 is required for cholesterol efflux by triggering histone demethylation, LXR recruitment, and coregulator assembly at the ABCG1 locus. *Mol Cell* 34: 510 – 518

Jiang C, Ito M, Piening V, Bruck K, Roeder RG, Xiao H (2004) TIP30 interacts with an estrogen receptor alpha-interacting coactivator CIA and regulates c-myc transcription. *J Biol Chem* 279: 27781 – 27789

Joseph SB, McKilligin E, Pei L, Watson MA, Collins AR, Laffitte BA, Chen M, Noh G, Goodman J, Hagger GN, Tran J, Tippin TK, Wang X, Lusis AJ, Hsueh WA, Law RE, Collins JL, Willson TM, Tontonoz P (2002) Synthetic LXR ligand inhibits the development of atherosclerosis in mice. *Proc Natl Acad Sci USA* 99: 7604 – 7609

Joseph SB, Castrillo A, Laffitte BA, Mangelsdorf DJ, Tontonoz P (2003) Reciprocal regulation of inflammation and lipid metabolism by liver X receptors. *Nat Med* 9: 213 – 219

Kariko K, Ni H, Capodici J, Lamphier M, Weissman D (2004) mRNA is an endogenous ligand for Toll-like receptor 3. *J Biol Chem* 279: 12542 – 12550

Khera AV, Cuchel M, de la Llera-Moya M, Rodrigues A, Burke MF, Jafri K, French BC, Phillips JA, Mucksavage ML, Wilensky RL, Mohler ER, Rothblat GH, Rader DJ (2011) Cholesterol efflux capacity, high-density lipoprotein function, and atherosclerosis. *N Engl J Med* 364: 127 – 135

Kim B, Nesvizhskii AI, Rani PG, Hahn S, Aebersold R, Ranish JA (2007) The transcription elongation factor TFIIS is a component of RNA polymerase II preinitiation complexes. *Proc Natl Acad Sci USA* 104: 16068 – 16073

Kinsella TM, Nolan GP (1996) Episomal vectors rapidly and stably produce high-titer recombinant retrovirus. *Hum Gene Ther* 7: 1405 – 1413

Lambert JP, Ivosev G, Couzens AL, Larsen B, Taipale M, Lin ZY, Zhong Q, Lindquist S, Vidal M, Aebersold R, Pawson T, Bonner R, Tate S, Gingras AC (2013) Mapping differential interactomes by affinity purification coupled with data-independent mass spectrometry acquisition. *Nat Methods* 10: 1239 – 1245

Lee S, Lee J, Lee SK, Lee JW (2008) Activating signal cointegrator-2 is an essential adaptor to recruit histone H3 lysine 4 methyltransferases MLL3 and MLL4 to the liver X receptors. *Mol Endocrinol* 22: 1312 – 1319

Lewis JP, Palmer ND, Ellington JB, Divers J, Ng MC, Lu L, Langefeld CD, Freedman BI, Bowden DW (2010) Analysis of candidate genes on chromosome 20q12-13.1 reveals evidence for BMI mediated association of PREX1 with type 2 diabetes in European Americans. *Genomics* 96: 211 – 219

Lundberg AM, Ketelhuth DF, Johansson ME, Gerdes N, Liu S, Yamamoto M, Akira S, Hansson GK (2013) Toll-like receptor 3 and 4 signalling through the TRIF and TRAM adaptors in haematopoietic cells promotes atherosclerosis. *Cardiovasc Res* 99: 364 – 373

Michelsen KS, Wong MH, Shah PK, Zhang W, Yano J, Doherty TM, Akira S, Rajavashisth TB, Arditi M (2004) Lack of Toll-like receptor 4 or myeloid differentiation factor 88 reduces atherosclerosis and alters plaque phenotype in mice deficient in apolipoprotein E. *Proc Natl Acad Sci USA* 101: 10679 – 10684

Mirzaei H, Knijnenburg TA, Kim B, Robinson M, Picotti P, Carter GW, Li S, Dilworth DJ, Eng JK, Aitchison JD, Shmulevich I, Galitski T, Aebersold R, Ranish J (2013) Systematic measurement of transcription factor-DNA interactions by targeted mass spectrometry identifies candidate gene regulatory proteins. *Proc Natl Acad Sci USA* 110: 3645 – 3650

Mittler G, Butter F, Mann M (2009) A SILAC-based DNA protein interaction screen that identifies candidate binding proteins to functional DNA elements. *Genome Res* 19: 284 – 293

Monaco C, Gregan SM, Navin TJ, Foxwell BM, Davies AH, Feldmann M (2009) Toll-like receptor-2 mediates inflammation and matrix degradation in human atherosclerosis. *Circulation* 120: 2462 – 2469

Moore KJ, Sheedy FJ, Fisher EA (2013) Macrophages in atherosclerosis: a dynamic balance. *Nat Rev Immunol* 13: 709 – 721

Mostafavi S, Ray D, Warde-Farley D, Grouios C, Morris Q (2008) GeneMANIA: a real-time multiple association network integration algorithm for predicting gene function. *Genome Biol* 9 (Suppl 1): S4

Mullick AE, Tobias PS, Curtiss LK (2005) Modulation of atherosclerosis in mice by Toll-like receptor 2. *J Clin Invest* 115: 3149 – 3156

Mullick AE, Soldau K, Kiosses WB, Bell TA 3rd, Tobias PS, Curtiss LK (2008) Increased endothelial expression of Toll-like receptor 2 at sites of disturbed blood flow exacerbates early atherogenic events. *J Exp Med* 205: 373 – 383

Neph S, Vierstra J, Stergachis AB, Reynolds AP, Haugen E, Vernot B, Thurman RE, John S, Sandstrom R, Johnson AK, Maurano MT, Humbert R, Rynes E, Wang H, Vong S, Lee K, Bates D, Diegel M, Roach V, Dunn D *et al* (2012) An expansive human regulatory lexicon encoded in transcription factor footprints. *Nature* 489: 83 – 90

Ogawa S, Lozach J, Benner C, Pascual G, Tangirala RK, Westin S, Hoffmann A, Subramaniam S, David M, Rosenfeld MG, Glass CK (2005) Molecular determinants of crosstalk between nuclear receptors and toll-like receptors. *Cell* 122: 707 – 721

Oram JF, Lawn RM, Garvin MR, Wade DP (2000) ABCA1 is the cAMP-inducible apolipoprotein receptor that mediates cholesterol secretion from macrophages. *J Biol Chem* 275: 34508 – 34511

Orso E, Broccardo C, Kaminski WE, Bottcher A, Liebisch G, Drobnik W, Gotz A, Chambenoit O, Diederich W, Langmann T, Spruss T, Luciani MF, Rothe G, Lackner KJ, Chimini G, Schmitz G (2000) Transport of lipids from golgi to plasma membrane is defective in tangier disease patients and Abc1-deficient mice. *Nat Genet* 24: 192 – 196

Paddison PJ, Cleary M, Silva JM, Chang K, Sheth N, Sachidanandam R, Hannon GJ (2004) Cloning of short hairpin RNAs for gene knockdown in mammalian cells. *Nat Methods* 1: 163 – 167

Pourfarzad F, Aghajanirefah A, de Boer E, Ten Have S, Bryn van Dijk T, Kheradmandkia S, Stadhouders R, Thongjuea S, Soler E, Gillemans N, von Lindern M, Demmers J, Philipsen S, Grosveld F (2013) Locus-specific proteomics by TChP: targeted chromatin purification. *Cell Rep* 4: 589 – 600

Rader DJ, Tall AR (2012) The not-so-simple HDL story: is it time to revise the HDL cholesterol hypothesis? *Nat Med* 18: 1344 – 1346

Ramsey SA, Klemm SL, Zak DE, Kennedy KA, Thorsson V, Li B, Gilchrist M, Gold ES, Johnson CD, Litvak V, Navarro G, Roach JC, Rosenberger CM, Rust AG, Yudkovsky N, Aderem A, Shmulevich I (2008) Uncovering a macrophage transcriptional program by integrating evidence from motif scanning and expression dynamics. *PLoS Comput Biol* 4: e1000021

Ramsey SA, Knijnenburg TA, Kennedy KA, Zak DE, Gilchrist M, Gold ES, Johnson CD, Lampano AE, Litvak V, Navarro G, Stolyar T, Aderem A, Shmulevich I (2010) Genome-wide histone acetylation data improve prediction of mammalian transcription factor binding sites. *Bioinformatics* 26: 2071 – 2075

Ranish JA, Yi EC, Leslie DM, Purvine SO, Goodlett DR, Eng J, Aebersold R (2003) The study of macromolecular complexes by quantitative proteomics. *Nat Genet* 33: 349 – 355

Ranish JA, Hahn S, Lu Y, Yi EC, Li XJ, Eng J, Aebersold R (2004) Identification of TFB5, a new component of general transcription and DNA repair factor IIH. *Nat Genet* 36: 707 – 713

Repa JJ, Turley SD, Lobaccaro JA, Medina J, Li L, Lustig K, Shan B, Heyman RA, Dietschy JM, Mangelsdorf DJ (2000) Regulation of absorption and ABC1-mediated efflux of cholesterol by RXR heterodimers. *Science* 289: 1524 – 1529

Richards MR, Black AS, Bonnet DJ, Barish GD, Woo CW, Tabas I, Curtiss LK, Tobias PS (2013) The LPS2 mutation in TRIF is atheroprotective in hyperlipidemic low density lipoprotein receptor knockout mice. *Innate Immun* 19: 20 – 29

Roach JC, Smith KD, Strobe KL, Nissen SM, Haudenschild CD, Zhou D, Vasicek TJ, Held GA, Stolovitzky GA, Hood LE, Aderem A (2007) Transcription factor expression in lipopolysaccharide-activated peripheral-blood-derived mononuclear cells. *Proc Natl Acad Sci USA* 104: 16245 – 16250

Rust S, Rosier M, Funke H, Real J, Amoura Z, Piette JC, Deleuze JF, Brewer HB, Duverger N, Denefle P, Assmann G (1999) Tangier disease is caused by mutations in the gene encoding ATP-binding cassette transporter 1. *Nat Genet* 22: 352 – 355

Sarachana T, Hu VW (2013) Differential recruitment of coregulators to the RORA promoter adds another layer of complexity to gene (dys) regulation by sex hormones in autism. *Mol Autism* 4: 39

Sauve F, McBroom LD, Gallant J, Moraitis AN, Labrie F, Giguere V (2001) CIA, a novel estrogen receptor coactivator with a bifunctional nuclear receptor interacting determinant. *Mol Cell Biol* 21: 343 – 353

Schultz JR, Tu H, Luk A, Repa JJ, Medina JC, Li L, Schwendner S, Wang S, Thoolen M, Mangelsdorf DJ, Lustig KD, Shan B (2000) Role of LXRs in control of lipogenesis. *Genes Dev* 14: 2831 – 2838

Sherwood RI, Hashimoto T, O'Donnell CW, Lewis S, Barkal AA, van Hoff JP, Karun V, Jaakkola T, Gifford DK (2014) Discovery of directional and nondirectional pioneer transcription factors by modeling DNase profile magnitude and shape. *Nat Biotechnol* 32: 171 – 178

Spann NJ, Garmire LX, McDonald JG, Myers DS, Milne SB, Shibata N, Reichart D, Fox JN, Shaked I, Heudobler D, Raetz CR, Wang EW, Kelly SL, Sullards MC, Murphy RC, Merrill AH Jr, Brown HA, Dennis EA, Li AC, Ley K *et al* (2012) Regulated accumulation of desmosterol integrates macrophage lipid metabolism and inflammatory responses. *Cell* 151: 138 – 152

Stewart CR, Stuart LM, Wilkinson K, van Gils JM, Deng J, Halle A, Rayner KJ, Boyer L, Zhong R, Frazier WA, Lacy-Hulbert A, El Khoury J, Golenbock DT, Moore KJ (2010) CD36 ligands promote sterile inflammation through

assembly of a Toll-like receptor 4 and 6 heterodimer. *Nat Immunol* 11: 155 – 161

Sun Z, Feng D, Fang B, Mullican SE, You SH, Lim HW, Everett LJ, Nabel CS, Li Y, Selvakumaran V, Won KJ, Lazar MA (2013) Deacetylase-independent function of HDAC3 in transcription and metabolism requires nuclear receptor corepressor. *Mol Cell* 52: 769 – 782

Tangirala RK, Bischoff ED, Joseph SB, Wagner BL, Walczak R, Laffitte BA, Daige CL, Thomas D, Heyman RA, Mangelsdorf DJ, Wang X, Lusis AJ, Tontonoz P, Schulman IG (2002) Identification of macrophage liver X receptors as inhibitors of atherosclerosis. *Proc Natl Acad Sci USA* 99: 11896 – 11901

Vaisman BL, Lambert G, Amar M, Joyce C, Ito T, Shamburek RD, Cain WJ, Fruchart-Najib J, Neufeld ED, Remaley AT, Brewer HB Jr, Santamarina-Fojo S (2001) ABCA1 overexpression leads to hyperalphalipoproteinemia and increased biliary cholesterol excretion in transgenic mice. *J Clin Invest* 108: 303 – 309

Venkateswaran A, Laffitte BA, Joseph SB, Mak PA, Wilpitz DC, Edwards PA, Tontonoz P (2000a) Control of cellular cholesterol efflux by the nuclear oxysterol receptor LXR alpha. *Proc Natl Acad Sci USA* 97: 12097 – 12102

Venkateswaran A, Repa JJ, Lobaccaro JM, Bronson A, Mangelsdorf DJ, Edwards PA (2000b) Human white/murine ABC8 mRNA levels are highly induced in lipid-loaded macrophages. A transcriptional role for specific oxysterols. *J Biol Chem* 275: 14700 – 14707

Viturawong T, Meissner F, Butter F, Mann M (2013) A DNA-centric protein interaction map of ultraconserved elements reveals contribution of transcription factor binding hubs to conservation. *Cell Rep* 5: 531 – 545

Wagner BL, Valledor AF, Shao G, Daige CL, Bischoff ED, Petrowski M, Jepsen K, Baek SH, Heyman RA, Rosenfeld MG, Schulman IG, Glass CK (2003) Promoter-specific roles for liver X receptor/corepressor complexes in the regulation of ABCA1 and SREBP1 gene expression. *Mol Cell Biol* 23: 5780 – 5789

Wang X, Collins HL, Ranalletta M, Fuki IV, Billheimer JT, Rothblat GH, Tall AR, Rader DJ (2007) Macrophage ABCA1 and ABCG1, but not SR-BI, promote macrophage reverse cholesterol transport in vivo. *J Clin Invest* 117: 2216 – 2224

Weintz G, Olsen JV, Fruhauf K, Niedzielska M, Amit I, Jantsch J, Mages J, Frech C, Dolken L, Mann M, Lang R (2010) The phosphoproteome of toll-like receptor-activated macrophages. *Mol Syst Biol* 6: 371

Xu XH, Shah PK, Faure E, Equils O, Thomas L, Fishbein MC, Luthringer D, Xu XP, Rajavashisth TB, Yano J, Kaul S, Arditi M (2001) Toll-like receptor-4 is expressed by macrophages in murine and human lipid-rich atherosclerotic plaques and upregulated by oxidized LDL. *Circulation* 104: 3103 – 3108

Yvan-Charvet L, Ranalletta M, Wang N, Han S, Terasaka N, Li R, Welch C, Tall AR (2007) Combined deficiency of ABCA1 and ABCG1 promotes foam cell accumulation and accelerates atherosclerosis in mice. *J Clin Invest* 117: 3900 – 3908

Yvan-Charvet L, Welch C, Pagler TA, Ranalletta M, Lamkanfi M, Han S, Ishibashi M, Li R, Wang N, Tall AR (2008) Increased inflammatory gene expression in ABC transporter-deficient macrophages: free cholesterol accumulation, increased signaling via toll-like receptors, and neutrophil infiltration of atherosclerotic lesions. *Circulation* 118: 1837 – 1847

Zervou MI, Goulielmos GN, Castro-Giner F, Boumpas DT, Tosca AD, Krueger-Krasagakis S (2011) A CD40 and an NCOA5 gene polymorphism confer susceptibility to psoriasis in a Southern European population: a case-control study. *Hum Immunol* 72: 761 – 765

Zhu X, Lee JY, Timmins JM, Brown JM, Boudyguina E, Mulya A, Gebre AK, Willingham MC, Hiltbold EM, Mishra N, Maeda N, Parks JS (2008) Increased cellular free cholesterol in macrophage-specific Abca1 knock-out mice enhances pro-inflammatory response of macrophages. *J Biol Chem* 283: 22930 – 22941

Zimmer S, Steinmetz M, Asdonk T, Motz I, Coch C, Hartmann E, Barchet W, Wassmann S, Hartmann G, Nickenig G (2011) Activation of endothelial toll-like receptor 3 impairs endothelial function. *Circ Res* 108: 1358 – 1366

